

Rapid and Precise Online Surface Reconstruction Method for Digital Modeling of Bulk Material Flow

Qiao, Wei; Hou, Chengcheng; Xiong, Xiaoyan; Dong, Huijie; Pang, Yusong; Yu, Junzhi

DOI

[10.1109/TII.2025.3538064](https://doi.org/10.1109/TII.2025.3538064)

Publication date

2025

Document Version

Final published version

Published in

IEEE Transactions on Industrial Informatics

Citation (APA)

Qiao, W., Hou, C., Xiong, X., Dong, H., Pang, Y., & Yu, J. (2025). Rapid and Precise Online Surface Reconstruction Method for Digital Modeling of Bulk Material Flow. *IEEE Transactions on Industrial Informatics*, 21(5), 4083-4093. <https://doi.org/10.1109/TII.2025.3538064>

Important note

To cite this publication, please use the final published version (if applicable).
Please check the document version above.

Copyright

Other than for strictly personal use, it is not permitted to download, forward or distribute the text or part of it, without the consent of the author(s) and/or copyright holder(s), unless the work is under an open content license such as Creative Commons.

Takedown policy

Please contact us and provide details if you believe this document breaches copyrights.
We will remove access to the work immediately and investigate your claim.




Green Open Access added to TU Delft Institutional Repository

'You share, we take care!' - Taverne project

<https://www.openaccess.nl/en/you-share-we-take-care>

Otherwise as indicated in the copyright section: the publisher is the copyright holder of this work and the author uses the Dutch legislation to make this work public.

Rapid and Precise Online Surface Reconstruction Method for Digital Modeling of Bulk Material Flow

Wei Qiao, Chengcheng Hou, Xiaoyan Xiong , Huijie Dong , *Member, IEEE*, Yusong Pang , and Junzhi Yu , *Fellow, IEEE*

Abstract—Digital twins and visual monitoring of conveyor systems require accurate digital models of dynamic bulk material flows, but existing methods struggle to achieve both speed and precision. This study develops a rapid online method to reconstruct dynamic bulk material flows on conveyor belts. First, a standardized online reconstruction scheme using visual detection of material flow contour lines is presented. Then, a feature detection algorithm is proposed to extract more refined points from laser line skeleton to accelerate the reconstruction process. An iterative-filtering interpolation algorithm that generates smooth interframe point clouds is introduced to improve mesh quality. Experimental results demonstrate that our method outperforms traditional corner detection-based reconstruction techniques in feature point detection, accuracy, mesh quality, and runtime performance. This research provides a practical solution for material handling digitalization, promoting the advancement of conveyor system digital twins and potentially improving operational efficiency and predictive maintenance in bulk material handling industries.

Index Terms—Belt conveyor, computer vision, digital model, digital twin (DT), dynamic material flow, online surface reconstruction.

I. INTRODUCTION

IN contemporary industry, belt conveyors serve as a crucial component of bulk material handling, and their efficiency and stability play a critical role in the seamless operation of entire production lines [1]. With ongoing advances in intelligentization and informatization, such as energy-saving speed regulation techniques for belt conveyors [2], [3], traditional monitoring methods struggle to meet the demands of efficient and intelligent production. As a key concept within Industry 4.0, digital twin (DT) technology enables continuous online monitoring, prediction, and optimization control by creating a virtual representation of physical entities in the digital realm [4], [5]. The application of DT technology to belt conveyors not only improves material handling efficiency and safety, but also reduces downtime through predictive maintenance, thereby minimizing operational costs [6].

Existing DT models for belt conveyors are primarily constructed based on readily detectable operational parameters and environmental conditions to predict and diagnose specific faults. For instance, Al-Kahwati et al. [7] developed a DT model for belt conveyors that enables the estimation of remaining useful life and degradation rates for certain components. Mafia et al. [8] designed a data connection and collection system, incorporating data from multiple sensors, to establish the data input for a belt conveyor DT model. Santos et al. [9] utilized infrared distance sensors and a three-axis accelerometer to measure belt rotation in pipe conveyors, employing an autoregressive language model to predict the overlap position of the conveyor belt. Pulcini and Modoni [10] proposed a machine learning-based DT system for conveyor belts, using various sensors to determine whether a belt failure has occurred. While these approaches have laid a crucial foundation for DT research oriented toward predictive maintenance, they have not considered the dynamic impact of material flow on belt conveyors, which is the most significant factor affecting these systems. To construct more advanced and precise DT models for belt conveyors, introducing digital models of dynamic material flow through online reconstruction as a new key input is essential. These newly incorporated digital

Received 11 May 2024; revised 23 August 2024 and 19 November 2024; accepted 24 January 2025. Date of publication 21 February 2025; date of current version 21 April 2025. This work was supported in part by the Science and Technology Major Project of Inner Mongolia under Grant 2021ZD0004 and in part by the Patent Conversion Special Plan of Shanxi Province under Grant 202305005. Paper no. TII-24-2267. (Corresponding author: Huijie Dong.)

Wei Qiao and Xiaoyan Xiong are with the College of Mechanical and Vehicle Engineering, Taiyuan University of Technology, Taiyuan 030024, China (e-mail: qiaowei0016@link.tyut.edu.cn; xiongxi-ayaoan@tyut.edu.cn).

Chengcheng Hou is with the Key Laboratory of Advanced Transducers and Intelligent Control System, Ministry of Education, Taiyuan University of Technology, Taiyuan 030024, China (e-mail: houchengcheng0203@link.tyut.edu.cn).

Huijie Dong is with the Key Laboratory of Advanced Transducers and Intelligent Control System, Ministry of Education, Taiyuan University of Technology, Taiyuan 030024, China, and also with the China Institute for Radiation Protection, Taiyuan 030024, China (e-mail: donghuijie@tyut.edu.cn).

Yusong Pang is with the Section of Transportation Engineering and Logistics, Department of Maritime and Transport Technology, Delft University of Technology, 2628CD Delft, The Netherlands (e-mail: y.pang@tudelft.nl).

Junzhi Yu is with the State Key Laboratory for Turbulence and Complex Systems, Department of Advanced Manufacturing and Robotics, BIC-ESAT, College of Engineering, Peking University, Beijing 100871, China (e-mail: junzhi.yu@ia.ac.cn).

This article has supplementary downloadable material available at <https://doi.org/10.1109/TII.2025.3538064>, provided by the authors.

Digital Object Identifier 10.1109/TII.2025.3538064

models of material flow can provide more detailed load distribution information and enable analysis of material characteristics and loading uniformity, which significantly influence equipment wear. This novel enhancement allows DT models to better simulate the interaction between materials and equipment components, ultimately achieving high-precision predictions of the remaining useful life for critical belt conveyor components.

The foundation for building digital models of dynamic material flow lies in the accurate detection of material flow surfaces. The current methods primarily consist of laser scanning and machine vision methods. In the laser scanning method, a laser scanner is predominantly employed to obtain the point cloud data. Zeng et al. [11] proposed a measurement model for bulk material flow based on laser scanning technology, where a laser scanner was utilized to capture the surface profile of the material on the conveyor belt. Similarly, Li et al. [12] obtained the 2-D profile of material flow using a laser scanner and combined it with a speed sensor to generate 3-D point cloud data of the material flow profile, further applying the Delaunay triangulation method for reconstruction. Miao et al. [13] employed two laser scanners to collect point cloud data from both the lower surface of the belt and the material surface, calculating cross sections and volume flows through matching processes. In the machine vision method, the point cloud is obtained by capturing a laser line stripe on the conveyor belt using a camera. Li et al. [14] used binocular vision to capture images above the laser line and calculated the cross-sectional area of the material at that line, which was then combined with belt speed to determine coal flow volume. Xu et al. [15] utilized a similar method for volume measurement and incorporated RFID technology to correct belt speed measurement. Qiao et al. [16] proposed a dual-field measurement scheme, in which two laser lines were captured by binocular cameras positioned at the upper and lower ends of the conveyor belt, enabling the acquisition of profile images of both upper and lower surfaces.

The digital models of dynamic material flow require precise and online surface reconstruction of the point cloud. However, the inherent dynamic and uncertain nature of material flow poses significant challenges to achieving online 3-D reconstruction. Existing methods mainly focus on utilizing point cloud data to calculate the volume of material flow. Due to the width of the laser line, dense point cloud data are obtained within each frame, with a significant portion being irrelevant to surface reconstruction purposes. Processing and recording such dense point clouds require substantial computational resources, storage space, and time, making it challenging to achieve online surface reconstruction in high-speed belt conveyor applications and subsequent predictive maintenance. Furthermore, data visualization is a crucial component for users interacting with DT systems [17]. The visualization of material flow can contribute to the augmented reality-assisted manufacturing or handling applications in a conveyor system [18], [19]. While surface reconstruction has been extensively applied in various fields for static point clouds [20], [21], the visualization of reconstructing dynamic point clouds representing material flows remains unexplored. Given these considerations, it is both valuable and necessary to generate accurate and refined point cloud data for dynamic

material flow and subsequently perform mesh generation for visualization purposes.

To build a high-fidelity digital model supporting the DT framework, this article presents a rapid online surface reconstruction method for bulk materials on a conveyor belt. The proposed method focuses on three crucial aspects that span different dimensions of the conveyor DT architecture: detection equipment and scheme within the physical entity layer; surface reconstruction method within the virtual equipment layer; visualization within the services layer. The contributions of this work are threefold as follows.

- 1) To build an online digital model, a standardized online surface reconstruction process based on the sequential profile lines of the material flow is proposed within a designed low-cost visual measurement scheme.
- 2) A novel laser line skeleton feature point detection algorithm is introduced. In comparison to traditional corner point detection algorithms, the proposed method can extract more accurate and fewer feature points to represent the laser line skeleton, thereby reducing the computations required for subsequent mesh generation.
- 3) An iterative-filtering interpolation algorithm is developed to generate smooth and representative interframe point clouds, enhancing the quality of the generated mesh.

Experimental results demonstrate the feasibility and effectiveness of the proposed online material flow surface reconstruction method. Compared to methods based on traditional corner detection algorithms, the proposed approach yields more refined and accurate feature points, enables faster overall surface reconstruction, and significantly improves mesh quality.

The rest of this article is organized as follows. Section II describes the low-cost material flow visual measurement scheme and the designed online reconstruction process. In Section III, an algorithm for extracting laser contour skeleton feature points is proposed. In Section IV, the point cloud interpolation algorithm and mesh generation algorithm are proposed. The experiments and analysis are performed in Section V. Finally, Section VI concludes this article.

II. ONLINE MATERIAL FLOW SURFACE RECONSTRUCTION SCHEME

A. Visual Measurement Scheme for Material Flow

To enhance the acquisition rate of material flow images, a material flow contour visual measurement scheme is designed, as shown in Fig. 1. This scheme employs a line light source in cooperation with a monocular camera, both of which are fixedly installed on the frame above the belt. The light source illuminates the material surface, forming a laser line perpendicular to the conveying direction. The camera is used to capture the contour line images of the material flow at the measurement position. In addition, a speed sensor is necessary to detect the instantaneous belt speed. In this scheme, the camera can acquire the material contour information on a single cross-section during each acquisition, and the 2-D actual coordinates of the contour are calculated through subsequent image processing. The position

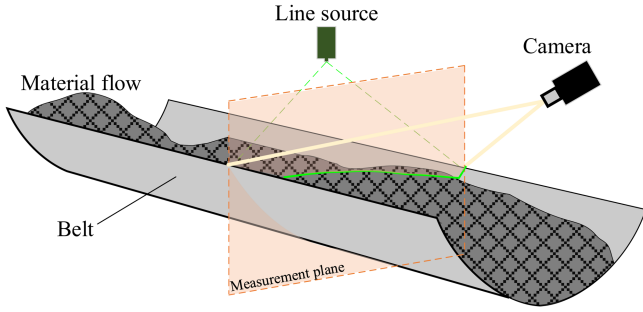


Fig. 1. Low-cost visual measurement scheme of the material flow.

of each cross section can be determined by calculating the acquisition moment and the instantaneous belt speed.

This scheme utilizes a monocular camera to reduce the size of the images that need to be processed, avoiding the time-consuming processes, such as image matching, which are commonly required when using binocular cameras. To maximize the accuracy and computational speed of the surface reconstruction, some physical constraints are imposed on the measurement scene in this article are as follows.

- 1) The installation positions of the camera and light source are relatively precise, with minimal vibration or offset during operation.
- 2) The ambient brightness is significantly darker than the brightness of the laser line, and the brightness distribution of the laser line is relatively uniform. The light source is less affected by dust and other disturbances.

While these constraints may seem challenging in some industrial environments, they can be effectively addressed through established engineering solutions. Precise positioning and vibration control can be achieved using robust mounting systems and vibration isolation techniques commonly employed in industrial imaging applications. To mitigate ambient light interference, strategies, such as high-power narrow-bandwidth lasers, optical filtering, and pulsed laser-camera synchronization, can be implemented to collect the image of laser line accurately and clearly.

B. Online Surface Reconstruction Process

The overall online surface reconstruction process is depicted in Fig. 2. The main steps include preprocessing, skeletonization, feature point detection, point cloud construction, point cloud interpolation, and meshing as follows.

- 1) First, during the preprocessing phase, after acquiring the original images, the binary image of the laser stripe is obtained through a series of image preprocessing steps, including region of interest (ROI) determination, grayscale conversion, image filtering, and binarization.
- 2) Second, based on the binary image, thinning and pruning are performed to extract the laser skeleton line.
- 3) Third, feature points are identified from the skeleton line, effectively using a small number of feature points to replace the skeleton line, thereby achieving downsampling while preserving critical features.

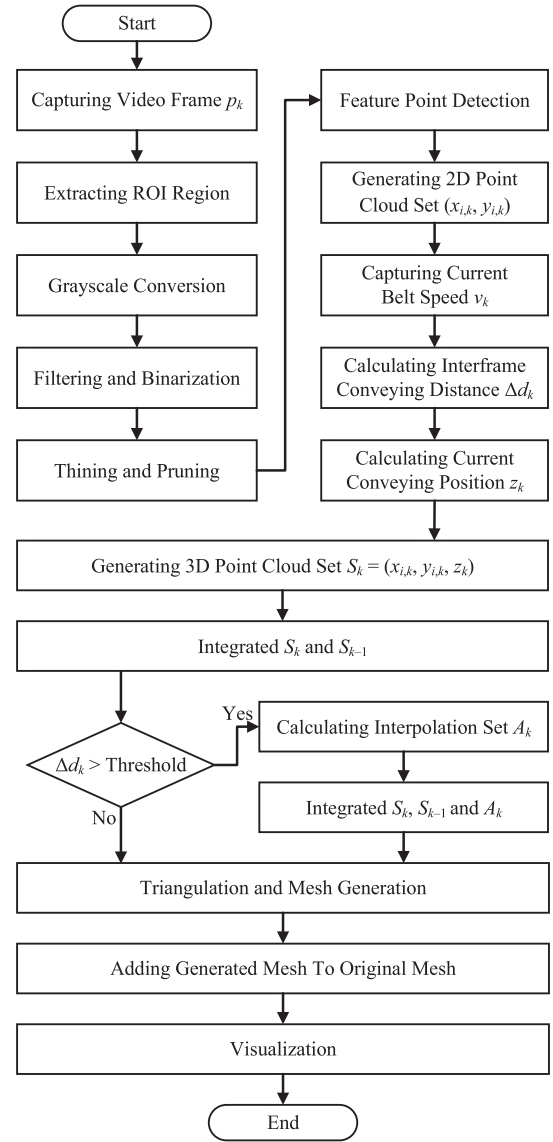


Fig. 2. Surface reconstruction process of bulk material flow by visual detection.

- 4) Fourth, using the feature points and belt speed data obtained in each frame, a refined 3-D point cloud is constructed.
- 5) Fifth, interpolation is applied to the point cloud at undetected positions based on the interframe distance, ensuring a complete representation of the surface.
- 6) Sixth, triangulation and mesh generation are performed. The newly generated mesh is seamlessly incorporated into the meshes produced during previous reconstruction processes.
- 7) Finally, the updated mesh information is visualized, providing an up-to-date representation of the reconstructed surface.

The above reconstruction process is mainly divided into image processing and point cloud processing stages. The objective of the image processing stage is to refine the feature points of

the laser line skeleton, which is based on image processing algorithms to extract key feature points from video frames to construct a key point cloud. The objective of the point cloud processing stage is to achieve rapid mesh reconstruction by interpolating and triangulating the refined point cloud to improve mesh performance. This article will illustrate the algorithms proposed for these two stages separately.

III. LASER LINE SKELETON FEATURE POINT DETECTION

To achieve surface reconstruction, the actual positions of the material flow contour points in each frame must be restored from the images to construct a point cloud. Since the points on the laser line stripe are generally not single-pixel points, extracting the centerline pixels of the line stripe as the actual detected contour line is essential. However, the extracted contour line still contains a large number of pixels, most of which are adjacent and collinear, leading to redundant calculations in subsequent 3-D reconstruction. To address this issue, this article proposes a laser line feature point detection algorithm that extracts a small number of feature points to replace the contour line, thereby reducing computational complexity.

The process of the proposed feature point detection algorithm for laser line stripe is shown in Fig. 3. First, the acquired image frame undergoes preprocessing to obtain a binary image of the contour. Then, through a thinning algorithm and pruning, an effective skeleton of the laser line stripe is obtained. Finally, the final feature points are determined through a series of filtering on the skeleton.

A. Image Preprocessing

First, based on the region where the contour line appears, the ROI is artificially defined to reduce the image size. Furthermore, a weighted average method is used to perform grayscale conversion on the image. Second, considering the influence of environmental lighting and other factors, noise exists in the image. A 3×3 window is used for median filtering to remove salt-and-pepper noise while preserving the edge information of the image. Finally, a binarization method is employed to convert the grayscale image into a black and white image. Since the ambient illumination is significantly darker than the brightness of the laser line, a global binarization with an empirical threshold can be used to save time. In the binarized image, white pixels represent the laser line, and black pixels represent the background, as shown in Fig. 3(b).

B. Thinning and Pruning

Since the laser line has a multipixel width, it is necessary to extract the contour skeleton from the foreground region. In this article, the Zhang–Suen thinning algorithm is used to process the binarized image, obtaining a contour skeleton with a single-pixel width. Furthermore, to address the possible occurrence of skeleton branches, which are often caused by the laser line illuminating the edges or gaps of the material, a pruning operation is required. Considering that the laser line located at the lower position on the same vertical position is definitely an

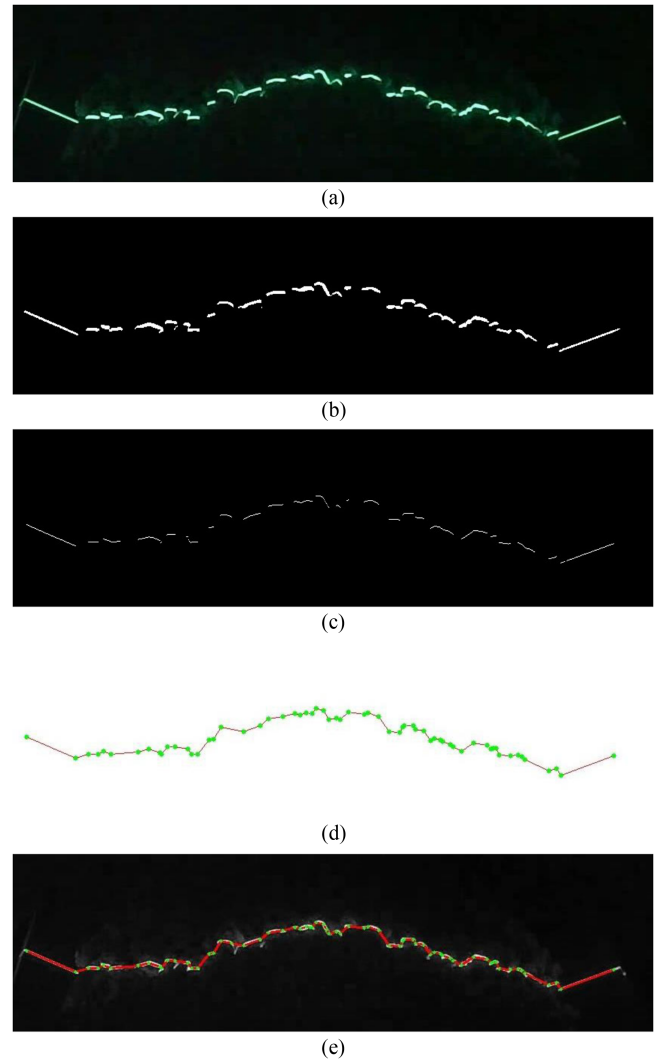


Fig. 3. Feature point detection process. (a) Original image. (b) Binarized image. (c) Skeleton image after thinning and pruning. (d) Detected feature points shown in green points and red lines. (e) Comparison of the detected feature points and the graying image.

interference, simple removal of points with the same horizontal coordinate and larger vertical coordinate in the image coordinate system can be performed, retaining only the skeleton at the upper part of the image. The result of this step are shown as Fig. 3(c), in which the foreground pixel value is 1 and the background pixel value is 0.

C. Feature Point Detection

After the above steps, most of the contour points obtained are pixel-adjacent. We aim to select the necessary feature points from them to accelerate the 3-D reconstruction process. These necessary feature points can be considered as the vertices of a series of connected line segments that can approximate the contour line. For the single-pixel contour line, the slope of its local points can only be 0° , $\pm 45^\circ$, or $\pm 90^\circ$. Therefore, it is difficult to obtain the desired results through traditional corner detection algorithms using only local information. On the other

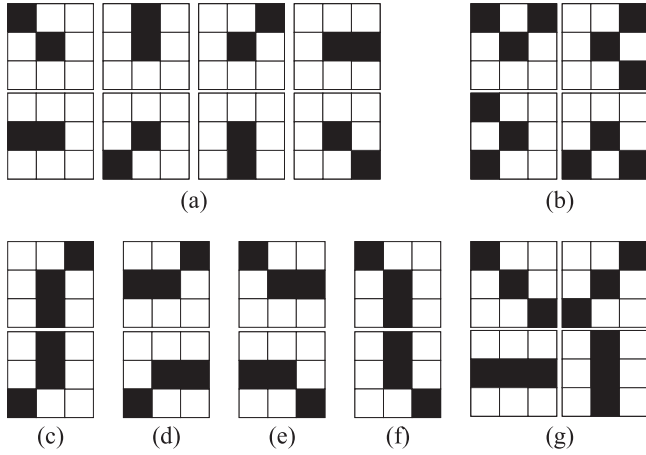


Fig. 4. Classification of foreground pixels in the skeleton image according to their eight-neighborhood. (a) Endpoints, $m = 9$. (b) Square points, $m = 8$. (c) Rising points with a large slope, $m = 7$. (d) Rising points with a smaller slope, $m = 5$. (e) Descending points with a smaller slope, $m = 3$. (f) Descending points with a larger slope, $m = 1$. (g) Collinear points, $m = 0$.

hand, the methods that calculate collinearity using large-scale information, such as curve fitting, will significantly increase the computational complexity. Consequently, we design a stepwise feature point detection algorithm that only utilizes local information, which includes three steps as illustrated in Algorithm 1.

Step 1: This step aims to reduce the number of points and obtain the local slope information of the remaining points. The points in the skeleton can be classified into endpoints, intermediate points, and isolated points. Endpoints have only one point in their eight-neighborhood, isolated points have no points in their eight-neighborhood, and intermediate points have two points in their eight-neighborhood. In this step, endpoints must be retained, while isolated points, which are usually interference points in the laser line, can be removed. The intermediate points are classified according to the distribution of their surrounding pixels to distinguish their slope information. Therefore, the following 3×3 convolution kernel is used to perform convolution on the image, and the above points are classified based on the convolution results. The convolution kernel is designed as

$$C_1 = \begin{bmatrix} 1 & 11 & 7 \\ 3 & 0 & 3 \\ 7 & 11 & 1 \end{bmatrix}. \quad (1)$$

Suppose the pixel value at the i th row and the j th column of the skeleton image is $p_{i,j}$, and its convolution result is $p_{i,j}^c$. The element $m_{i,j}$ at the corresponding position of a new matrix M is defined as

$$m_{i,j} = \begin{cases} 9, & p_{i,j} = 1, p_{i,j}^c \text{ is odd} \\ 8, & p_{i,j} = 1, p_{i,j}^c = 8 \\ 7, & p_{i,j} = 1, p_{i,j}^c = 18 \\ 5, & p_{i,j} = 1, p_{i,j}^c = 10 \\ 3, & p_{i,j} = 1, p_{i,j}^c = 4 \\ 1, & p_{i,j} = 1, p_{i,j}^c = 12 \\ 0, & \text{others.} \end{cases} \quad (2)$$

Algorithm 1: Feature point detection algorithm from skeleton image.

Input: P – Skeleton image

c_2, c_{31}, c_{32} – Filtering coefficients

Output: S_3 – List of detected feature points

Step 1

1: Create a zero matrix M with the same size as the input image

2: Use the kernel C to perform a convolution operation on P

3: Assign element in M a value according to equation (2)

Step 2

4: Extract coordinates (x_k, y_k) of the nonzero elements in M column-wise, and define

$$S_1(k) = (x_k, y_k)$$

5: For $k = 1, 2, 3, \dots$, do:

6: If $m_{x_k, y_k} = 9$, or $m_{x_k, y_k} \neq m_{x_{k-1}, y_{k-1}}$ and $d_{1,k} > k_2$

7: Then define $S_1(k)$ as a retained point

8: Else define $S_1(k)$ as a removed point

9: Save all retained point in S_1 to an array S_2

Step 3

10: Define the first and last points in S_2 as the retained points

11: For $k = 1, 2, 3, \dots$, do:

12: If $d_{2,k} \geq k_3$ or $d_{3,k} \geq k_3$

13: Then define $S_2(k)$ as a retained point

14: Else define $S_2(k)$ as a removed point

15: Save all retained point in S_2 to an array S_3

16: Return S_3

As shown in Fig. 4, after this convolution, the foreground pixels in the skeleton image are divided into seven categories, where the point with $m_{i,j} = 9$ corresponds to the endpoint and $m_{i,j} = 8$ corresponds to the square point. Points with different slopes correspond to $m_{i,j} = 7, 5, 3$, or 1 . In addition, collinear points and scattered points are unnecessary, and the corresponding positions in M are assigned a value of 0 .

Step 2: Remove the points with the same slope parameter as their adjacent points or the points that are close to the retained points. In this step, the row and column positions of nonzero elements from the matrix M are extracted column by column from left to right to obtain the sequence $S_1 = (x_k, y_k) | m_{x_k, y_k} \neq 0$. A single loop is performed on S_1 to determine whether a point should be removed or retained. Points satisfying $m_{x_k, y_k} \neq 9$ and $m_{x_k, y_k} = m_{x_{k-1}, y_{k-1}}$ are removed. In addition, points satisfying $d_{1,k} < c_2$ are removed, where $d_{1,k}$ represents the Manhattan distance between $S_1(k)$ and the last retained point. After this loop, the sequence S_2 is obtained. Through this step, the number of skeleton points can be significantly reduced based on local slope information.

Step 3: Remove points that are approximately on the line connecting their neighbor points. In a loop traversing all points in S_2 , the points satisfying $d_{2,k} < c_{31}$ and $d_{3,k} < c_{32}$ are removed

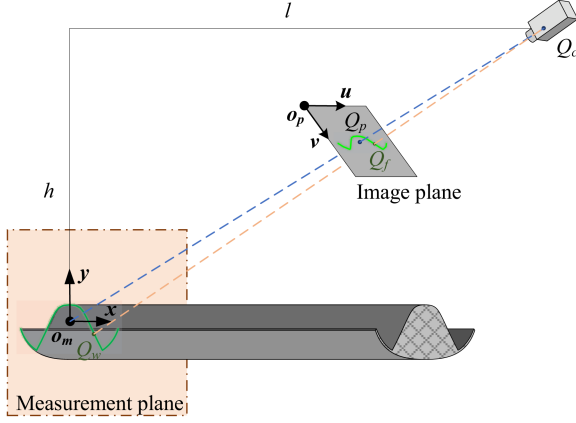


Fig. 5. Relative position of the camera and the measurement plane.

to construct an array S_3 , where $d_{2,k}$ represents the distance between $S_2(k)$ and the line connecting the last retained point and $S_2(k+1)$, and $d_{3,k}$ represents Manhattan distance between $S_2(k)$ and the last retained point. Finally, the points in S_3 are regarded as the detected feature points of the skeleton image.

Among the three filtering parameters, c_2 is used to remove points that are too close to each other. A smaller value of c_2 results in denser feature points; conversely, a larger value leads to sparser feature points, but useful feature points may be lost. c_{31} is used to determine the degree of collinearity with neighboring points, while c_{32} is used to retain relatively sparse points. The values of these parameters can be set according to the specific requirements of the application.

The finally detected feature points are shown in Fig. 3(d), where the green points represent the feature points and the red lines are the connecting lines between adjacent feature points. Fig. 3(e) illustrates the accuracy and performance of the detected feature points. The more the green points and red lines cover the region of the laser line, the more accurate the detection is considered to be. In addition, a smaller number of points indicates better refining performance.

IV. POINT CLOUD DATA PROCESSING AND MESH GENERATION

The obtained refined feature points can be converted to 3-D point clouds through projective transformation. It should be noted that the original point cloud is only located at the actual detected positions on the material flow surface, which are related to belt speed and frame rate. Thus, the point cloud data need to be interpolated at other undetected positions to achieve better mesh quality. In this section, the proposed point cloud interpolation algorithm and mesh generation process are illustrated.

A. Point Cloud Construction

The detection coordinate system is shown in Fig. 5. According to the projective transformation principle, a pixel Q_f on the image must correspond to a point Q_w on the measurement plane. Thus, all detected feature points can be transferred to 2-D point cloud data on the measurement plane based on the camera model.

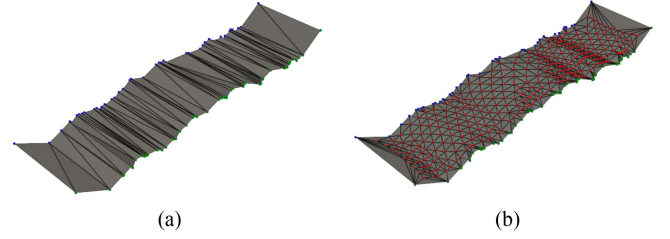


Fig. 6. Point cloud interpolation for high belt speed. (a) Mesh generated directly from feature points. (b) Mesh generated after interpolation.

Suppose that the coordinate set on the measurement plane of the feature points at the k th time is $\{(x_{k,i}, y_{k,i}) | i \in (1, n_k)\}$, where n_k is the number of feature points. The z -axis position of the current measurement plane on the conveyor belt is $z_k = z_{k-1} + v_k t_k$, where v_k is the current instantaneous belt speed and t_k is the current image acquisition time interval. Then, the 3-D point cloud set obtained from the k th acquisition is $P_k = \{(x_{k,i}, y_{k,i}, z_k) | i = 1, 2, \dots, n_k\}$.

B. Point Cloud Interpolation

Since detection is performed only on the measurement plane, the 3-D point cloud obtained each time is coplanar. When the belt speed is high, the interval length between adjacent frames may be relatively large, resulting in an overly sparse point cloud and a deterioration in the mesh quality of surface reconstruction, as illustrated in Fig. 6. Considering that a uniform point cloud generates meshes of good quality, this article proposes an iterative-filtering linear interpolation method. The point cloud sets obtained from current and previous frames are denoted as $P_c = \{(x_c, y_c, z_c)\}$ and $P_p = \{(x_p, y_p, z_p)\}$, respectively. Their separate numbers of points are n_c and n_p . First, the number of interpolation planes n_z is calculated based on the maximal distance threshold parameter z_d as

$$n_z = \left\lfloor \frac{z_c - z_p}{z_d} \right\rfloor \quad (3)$$

where $\lfloor \cdot \rfloor$ represents the flooring function. By setting the even-distributed interpolation plane, the z coordinate z_i of the interpolated point set P_i in each plane is

$$z_i = z_p + i \cdot \frac{z_c - z_p}{n_z + 1}, i = 1, 2, \dots, n_z. \quad (4)$$

The interpolated points are calculated for interpolated planes in turns. First, for each interpolation point set P_i , the weight coefficient $w_{c,i}$ referring to P_c and the weight coefficient $w_{i-1,i}$ referring to last interpolation plane P_{i-1} are defined as

$$w_{c,i} = \frac{1}{n_z - i + 2} \quad (5)$$

$$w_{i-1,i} = 1 - w_{c,i}. \quad (6)$$

Specifically, P_0 is identical to P_p . We define the point set $P_{i-1,c}$ as the mixture of P_{i-1} and P_c sorted according to the x -axis. The weight coefficient set $\Omega_{i-1,c}$ is defined as the mixture of weight coefficients corresponding to $P_{i-1,c}$. In other words,

if $P_{i-1,c}(j)$ originates from P_{i-1} , then $\Omega_{i-1,c}(j) = w_{i-1,i}$; conversely, if $P_{i-1,c}(j)$ originates from P_c , then $\Omega_{i-1,c}(j) = w_{c,i}$.

Then, the interpolation point in P_i is obtained as

$$x_{i,j} = \frac{x_{i-1,j}w_j + x_{i-1,j+1}w_{j+1}}{w_j + w_{j+1}}, j = 1, \dots, n_{i-1} + n_c - 1 \quad (7)$$

$$y_{i,j} = \frac{y_{i-1,j}w_j + y_{i-1,j+1}w_{j+1}}{w_j + w_{j+1}}, j = 1, \dots, n_i + n_e - 1. \quad (8)$$

During each iteration, two additional filtering operations are applied to remove redundant points. First, the points with $w_j + w_{j+1} < 1$ are removed. Second, if the Euclidean distance between two adjacent interpolation points is less than a threshold c_f , their median point is used to replace the two points. This iteration with filtering is repeated until the n_z interpolation point sets are completed.

Compared with direct linear interpolation, the above algorithm is characterized by the dual filtering mechanism. The weight-based filtering serves to eliminate unreliable or poorly supported interpolated points. The distance-based filtering prevents overcrowding of points in certain areas, which could lead to mesh irregularities. These filtering processes contribute to noise and outlier reduction, promote a more uniform point distribution, and mitigate the accumulation of interpolation errors.

C. Mesh Generation

Transforming scattered point cloud data into a continuous surface model is necessary for digital modeling and visual representation. Considering that the generated point cloud is arranged in order, the commonly used Delaunay triangulation method is employed for surface reconstruction. To accelerate the triangulation process, the 3-D points are first mapped onto the oyz plane. Then, the triangular mesh is constructed according to the rules of Delaunay triangulation, and finally, the mesh is mapped back to the corresponding 3-D positions.

Since the point cloud data are computed online frame by frame, the online process of surface reconstruction is described as follows.

- 1) Detect the feature points in the current frame and calculate the 3-D point set.
- 2) Read the 3-D point set obtained from the previous frame.
- 3) Perform point cloud interpolation to obtain the supplemented point set.
- 4) Perform Delaunay triangulation using the y and z coordinates of the point cloud.
- 5) Add the obtained mesh to the existing mesh.

V. RESULTS AND ANALYSIS

An experimental system was constructed based on the proposed reconstruction scheme for validation. The experimental conveyor is 5-m long and has a belt width of 800 mm. The material being transported is gravel with diameters ranging from 1 to 2 cm. A green line laser with an output power of 30 mW was employed. The camera has a resolution of 1280×720 and

a capture frequency of 60 fps. The ROI size is designated as 850×500 . An Intel Core i9-12900K CPU with a base frequency of 3.19 GHz was used for all computation, which operates on Windows 10, and the compilation environment is Python. OpenCV library was used for image processing, Scipy.spatial library for Delaunay triangulation computation, and skimage.morphology for image thinning operations. The proposed algorithm code was implemented based on NumPy. The coefficients are set as $(c_2, c_{31}, c_{32}, c_f) = (2, 0.5, 30, 10)$. First, the effectiveness and computational efficiency of the proposed feature point extraction algorithm were tested. Then, comparisons and analyses of the reconstruction results are presented.

A. Feature Point Detection Results

To validate the effectiveness of the proposed feature point extraction algorithm, it is compared with existing corner detection algorithms, including Harris and FAST algorithms, which were implemented by OpenCV library in Python. The comparison is conducted in terms of the number of extracted feature points, error, and computational time. The error is defined as the absolute value of the area enclosed by the curve formed by connecting the extracted feature points and the thinned contour line, to characterize the ability of the extracted feature points to represent the contour line. In total, ten experimental videos, consisting of 3805 image frames, were used for the calculations and statistics. Some feature point extraction results are shown in the Fig. 7, and the statistical results are presented in the Table I.

As illustrated in the Fig. 7, the green dots represent the extracted feature points, and the red lines connect adjacent feature points. The background is the gray image, where white area represents the captured laser line. Therefore, the more the white area is covered, the more accurate the extracted feature points are. It can be observed that the results of the FAST algorithms clearly show the most laser lines that are not covered, indicating the abundant loss of effective feature points and inadequacy for feature point detection of the laser skeleton image. For the Harris algorithm, the accuracy of the detected feature points is better but the quantity is overmuch.

In contrast, the proposed method achieves more precise feature point detection. The statistical results in Table I show that the refining rate of the proposed method is only 11.18%. Moreover, the error area of the proposed method is significantly smaller than other algorithms. The results indicate that the proposed method possesses superior refining performance to detect feature points of laser skeleton.

B. Online Surface Reconstruction With Low Belt Speed

In this part, surface reconstruction under low-speed operating conditions is performed to analyze the mesh quality and computational efficiency of the proposed method. The material flow in ten transportation processes was completely reconstructed. The belt speed was set to 1.2 m/s, and the transportation distance between frames was 20 mm. The interframe distance is short so that the interpolation algorithm was not employed. A single-threaded programming strategy was used to complete the extraction of feature points from video frames, the processing of point clouds,

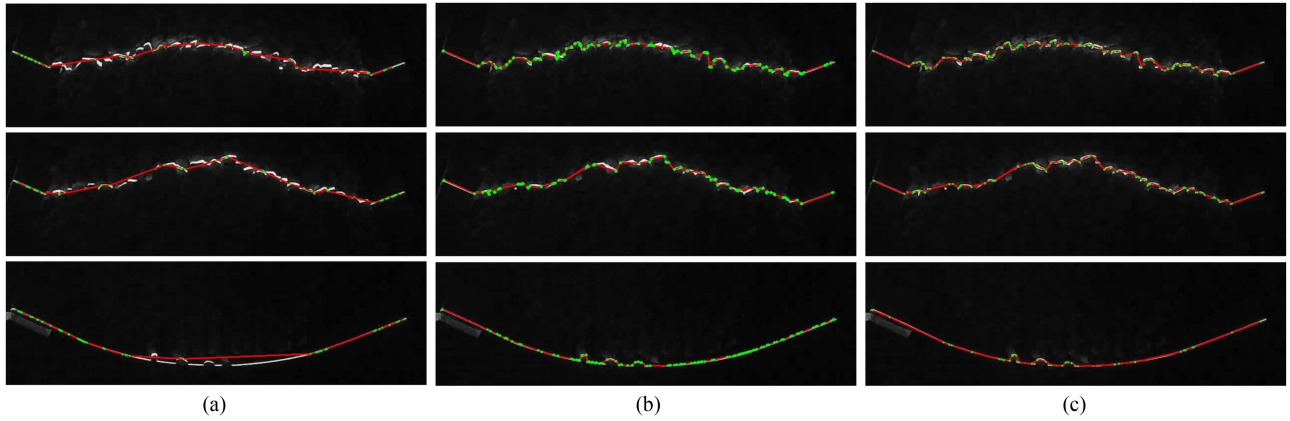


Fig. 7. Comparison of detected feature points in three selected frames. (a) FAST algorithm. (b) Harris algorithm. (c) Our proposed algorithm.

TABLE I
STATISTICS AND COMPARISON OF FEATURE POINT DETECTION RESULT

Item	Our proposed algorithm	Harris algorithm	FAST algorithm
Number of skeleton pixel	482.16 ± 89.05	482.16 ± 89.05	482.16 ± 89.05
Number of feature points	53.91 ± 18.45	169.26 ± 47.25	44.07 ± 10.77
Error (mm^2)	667.67 ± 443.89	1434.32 ± 547.95	3471.09 ± 1437.87
Time consumption (ms)	10.55 ± 1.33	5.28 ± 1.02	0.25 ± 0.09

TABLE II
STATISTICAL RESULTS OF ONLINE SURFACE RECONSTRUCTION AT LOW BELT SPEED

Item	Our proposed reconstruction method	Harris-based reconstruction method
Number of frames	37.80 ± 0.42	37.80 ± 0.42
Processing time per frame (ms)	23.65 ± 0.44	32.65 ± 1.42
Feature point number	2037.00 ± 125.29	$15\,503.70 \pm 870.37$
Mesh number	3951.60 ± 241.69	$30\,064.90 \pm 1770.43$

and mesh generation. The number of triangular meshes, size distribution, and processing time of each frame were statistically analyzed, and the reconstruction results obtained by the Harris method were compared with those obtained by feature point triangulation. The FAST algorithm was not utilized in this part due to the unrepresentative nature of the detected feature points for material flow surfaces.

The reconstruction results in one test are presented in Fig. 8. The material is gravel of 70 kg and the total conveying distance is 740 mm. The mesh regions with different height are distinguished with different colors. In the results obtained by the proposed method, there are fewer mesh shadows near feature points compared to those obtained by other methods, indicating less elongated meshes and better mesh quality.

The statistical results of ten video reconstructions are presented in Table II. The frame count of each video was approximately 37.8 frames. In the results of the Harris method, the average number of feature points per frame was 410.15, while the number for the proposed method was 53.89, only 13.14% of the last value. In addition, the total time consumed to detect the feature points and generate meshes for a single frame was

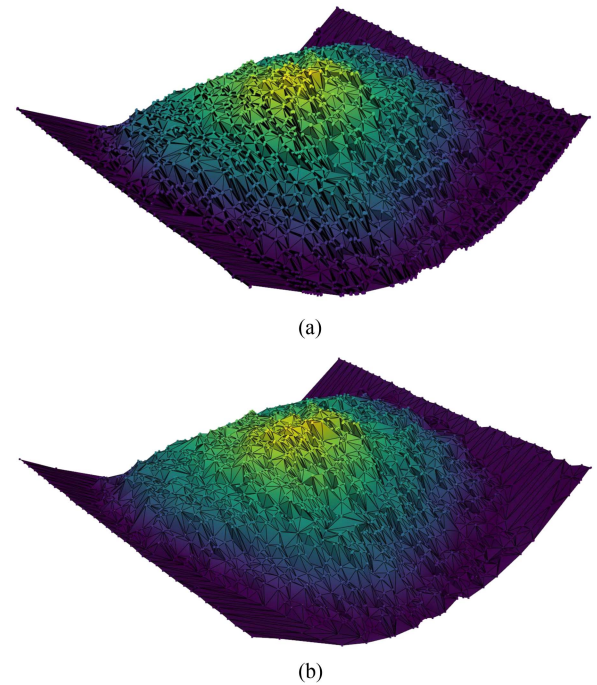


Fig. 8. Comparison of surface reconstruction results at low belt speeds. (a) Reconstruction based on Harris corner detection. (b) Proposed method.

approximately 23.65 ms, which is 27.57% faster than that of the Harris method.

To analyze the quality of the mesh, the aspect ratio of the triangular mesh was statistically analyzed, as shown in Fig. 9. In this article, the aspect ratio of a triangular mesh is defined as

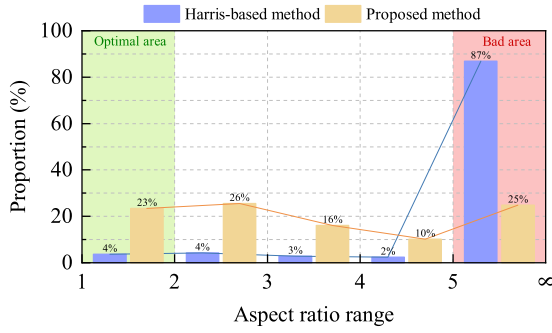


Fig. 9. Aspect ratio statistics of the generated triangular mesh.

the ratio of the longest side to the shortest height of the triangle, with a range of $[2/\sqrt{3}, +\infty)$. The optimal triangular grid is an equilateral triangle, with a minimal aspect ratio, approximately equal to 1.15. The larger the aspect ratio, the more elongated the triangle becomes. Triangular grids with aspect ratios less than 2.0 can be considered high-quality grids, while triangular grids with aspect ratios greater than 5 are considered poor grids. It can be observed from Fig. 9 that among the meshes obtained by the Harris method, high-quality meshes only account for 4%, and poor meshes account for 84%. However, the method proposed in this article yielded up to 23% high-quality meshes and 25% poor meshes, demonstrating a significant improvement compared to the conventional reconstruction method.

C. Online Surface Reconstruction With High Belt Speed

In this part, surface reconstruction under high-speed operating conditions is further performed. The material flow in ten transportation processes was completely reconstructed. The simulated belt speed was set to 6 m/s, meaning that the transportation distance between frames was 100 mm. The interpolation interval was set to 20 mm. The programming strategy was the same as the low-speed experiments but the interpolation algorithm was enabled.

The reconstruction results for 20 frames are presented in Fig. 10. The red dots represent the detected feature points, while the others are interpolation points. In the results obtained by the proposed method, there are fewer mesh shadows near feature points compared to those obtained by other methods, indicating better mesh quality. Although the feature points obtained by the Harris method are relatively dense, the grids in the interpolation part are significantly sparser and more uniform, which demonstrates that the proposed interpolation method can effectively improve the mesh quality.

The statistical results of ten video reconstructions are presented in Table III. The frame count of each video is approximately 381 frames. In the results of the proposed method, the average number of feature points per frame was 54.45, and the number of points per interpolation row was 35.81, which accounted for 65.77% of the total. The corresponding data for the Harris method were 412.25, 29.40, and 7.13%, respectively. The number of interpolation points was less than the number of feature points, suggesting that the validity of the points generated

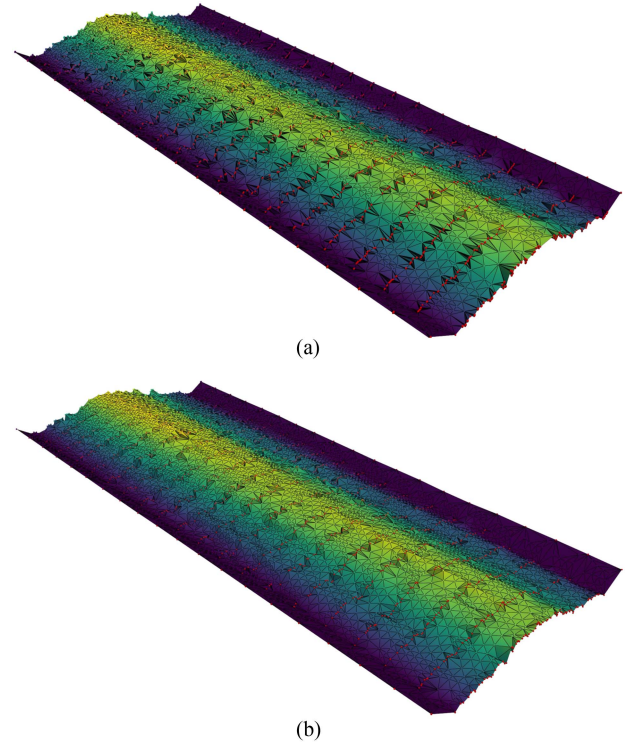


Fig. 10. Comparison of surface reconstruction results at high belt speeds. (a) Reconstruction based on Harris corner detection. (b) Proposed method.

TABLE III
STATISTICAL RESULTS OF ONLINE SURFACE RECONSTRUCTION AT HIGH BELT SPEED

Item	Our proposed reconstruction method	Harris-based reconstruction method
Number of frames	381.10 ± 2.18	381.10 ± 2.18
Processing time per frame (ms)	24.09 ± 0.42	33.23 ± 0.84
Feature point number	20 750.00 ± 861.44	157 108.50 ± 3842.99
Interpolated point number	54 583.50 ± 764.52	44 812.20 ± 405.32
Triangular mesh number	149 865.50 ± 3047.43	401 802.30 ± 7849.82

by the proposed interpolation algorithm was superior. The total time consumed for a single frame is approximately 24.09 ms, which is 27.5% faster than that of the Harris method.

The aspect ratio of the triangular mesh was also statistically analyzed as shown in Fig. 11. It can be observed that among the meshes obtained by the Harris method, high-quality meshes only account for 16%, and poor meshes account for 69%. However, the method proposed in this article yielded up to 50% high-quality meshes and only 9% poor meshes, demonstrating a significant improvement compared to the conventional reconstruction method.

D. Discussion

The above experimental results indicate that the proposed innovative online surface reconstruction method has the characteristics of high computation efficiency and intuitiveness, which

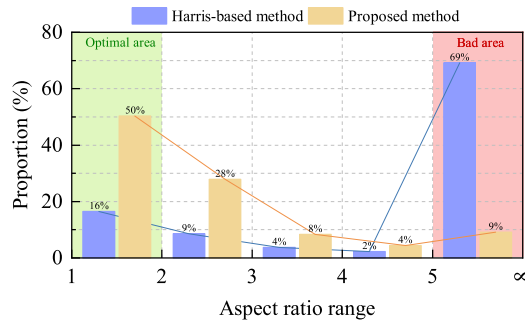


Fig. 11. Aspect ratio statistics of the generated triangular mesh.

can generate intuitive and vivid visualization effects of material transportation, enabling a more intuitive understanding of the operating status of the conveyor and improve the management and scheduling efficiency of the conveyor.

The proposed method does not increase computational complexity in the feature detection process compared to the Harris algorithm, as its most complex operation is a 3×3 convolution on the image. However, our algorithm generates significantly fewer points in the point cloud, thereby substantially reducing the complexity of the triangulation process. The combination of maintained efficiency in feature detection and reduced complexity in triangulation allows our method to achieve superior computational speed while maintaining high-quality surface reconstruction.

In our experiments, the number of feature points obtained by our algorithm was approximately 13% of those obtained by the Harris algorithm, demonstrating the effectiveness of our method in reducing data redundancy. The refined data significantly reduce the storage space and bandwidth requirements for data recording. Furthermore, the triangulated mesh digital model generated by the algorithm contains valuable spatial information about the material. Thus, our algorithm contributes to improving the overall efficiency of predictive maintenance in conveyor belt systems.

Despite the good performance of the proposed reconstruction method, the experimental environment was designed to be rayless to accentuate the laser line, thereby simplifying the laser line skeleton extraction process. An accurate skeleton is the premise for subsequent surface reconstruction. Therefore, an arrangement to reduce disturbance from environmental light may be required. In addition, specific optimizations in image preprocessing may also be beneficial.

VI. CONCLUSION AND FUTURE WORK

This article proposes a rapid online surface reconstruction method addressing the demand for high-fidelity material flow digital modeling. First, a standardized online surface reconstruction process based on sequential profile lines of material flow is presented, implemented within a low-cost visual measurement scheme. Second, a novel laser line skeleton feature point detection algorithm for constructing refined point clouds is proposed. Third, an iterative-filtering interpolation algorithm is developed

to generate smooth and representative interframe point sets, enhancing mesh quality. Experimental results demonstrate the feasibility and effectiveness of our proposed method. Compared to methods based on traditional corner detection algorithms, the proposed approach yields more refined and accurate feature points, enables faster overall surface reconstruction, and significantly improves mesh quality. Particularly, the proposed method achieves a refining rate of 11.18% with less area error, which is substantially superior to the 35.1% rate of the Harris algorithm. In the entire reconstruction, our method enhances computational speed by 27.5% compared to the Harris method. The refined data also significantly reduce the storage space and bandwidth requirements for data recording, which contributes to improving the overall efficiency of predictive maintenance in conveyor belt systems. This work can provide a solid foundation for developing more efficient and reliable digital modeling systems in industrial material handling applications, potentially transforming how bulk material transportation is monitored and maintained.

Our future work will focus on enhancing the information dimension of the virtual material flow model through multisource information perception and fusion to extend the digital model's functionality. We will also further develop a comprehensive DT framework that incorporates our surface reconstruction method with other key aspects of conveyor belt operations, such as predictive maintenance and energy optimization.

REFERENCES

- [1] B. Bolat, B. A. Temiztas, E. Sezer, and A. Solak, "Investigation of numerical belt sag and conveyor capacities in inclined belt conveyors: An iterative approach," *Powder Technol.*, vol. 420, 2023, Art. no. 118394.
- [2] L. B. Ristic and B. I. Jeftenic, "Implementation of fuzzy control to improve energy efficiency of variable speed bulk material transportation," *IEEE Trans. Ind. Electron.*, vol. 59, no. 7, pp. 2959–2969, Jul. 2012.
- [3] D. He, Y. Pang, G. Lodewijks, and X. Liu, "Healthy speed control of belt conveyors on conveying bulk materials," *Powder Technol.*, vol. 327, pp. 408–419, 2018.
- [4] M. Schluse, M. Priggemeyer, L. Atorf, and J. Rossmann, "Experimentable digital twins-streamlining simulation-based systems engineering for industry 4.0," *IEEE Trans. Ind. Inf.*, vol. 14, no. 4, pp. 1722–1731, Apr. 2018.
- [5] F. Tao, H. Zhang, A. Liu, and A. Y. C. Nee, "Digital twin in industry: State-of-the-Art," *IEEE Trans. Ind. Inf.*, vol. 15, no. 4, pp. 2405–2415, Apr. 2019.
- [6] G. Fedorko, V. Molnar, M. Vasil, and R. Salai, "Proposal of digital twin for testing and measuring of transport belts for pipe conveyors within the concept industry 4.0," *Measurement*, vol. 174, 2021, Art. no. 108978.
- [7] K. Al-Kahwati, W. Birk, E. F. Nilsfors, and R. Nilsen, "Experiences of a digital twin based predictive maintenance solution for belt conveyor systems," in *Proc. PHM Soc. Eur. Conf.*, 2022, pp. 1–8.
- [8] M. M. P. Mafia, N. Ayoub, L. Trumpler, J. P. de, and O. Hansen, "A digital twin design for conveyor belts predictive maintenance," in *Machine Learning for Cyber-Physical Systems*, 1st ed. Berlin, Germany: Springer, 2023, pp. 111–119.
- [9] L. D. S. e Santos, P. R. C. F. Ribeiro Filho, and E. N. Macedo, "Belt rotation in pipe conveyors: Development of an overlap monitoring system using digital twins, industrial Internet of Things, and autoregressive language models," *Measurement*, vol. 230, Art. no. 114546, 2024.
- [10] V. Pulcini and G. Modoni, "Machine learning-based digital twin of a conveyor belt for predictive maintenance," *Int. J. Adv. Manuf. Technol.*, vol. 133, pp. 6095–6110, 2024.
- [11] F. Zeng, Q. Wu, X. Chu, and Z. Yue, "Measurement of bulk material flow based on laser scanning technology for the energy efficiency improvement of belt conveyors," *Measurement*, vol. 75, pp. 230–243, 2015.

- [12] Z. Li, Q. Wu, F. Zeng, and Z. Yue, "3D reconstruction of material transportation status on belt conveyors," in *Proc. Int. Comput. Conf. Wavelet Act. Media Technol. Inf. Process.*, Chengdu, China, 2015, pp. 168–172.
- [13] D. Miao, Y. Wang, L. Yang, and S. Wei, "Coal flow detection of belt conveyor based on the two-dimensional laser," *IEEE Access*, vol. 11, pp. 82294–82301, 2023.
- [14] J. Li, J. Zhang, H. Wang, and B. Feng, "Coal flow volume measurement of belt conveyor based on binocular vision and line structured light," in *Proc. IEEE Int. Conf. Elect. Eng. Mechatron. Technol.*, Qingdao, China, 2021, pp. 636–639.
- [15] S. Xu, G. Cheng, Z. Cui, Z. Jin, and W. Gu, "Measuring bulk material flow—incorporating RFID and point cloud data processing," *Measurement*, vol. 200, 2022, Art. no. 111598.
- [16] W. Qiao, Y. Lan, H. Dong, X. Xiong, and T. Qiao, "Dual-field measurement system for real-time material flow on conveyor belt," *Flow Meas. Instrum.*, vol. 83, 2022, Art. no. 102082.
- [17] A. Sigov, L. Ratkin, L. A. Ivanov, and L. D. Xu, "Emerging enabling technologies for industry 4.0 and beyond," *Inf. Syst. Front.*, vol. 26, pp. 1585–1595, 2022, doi: [10.1007/s10796-021-10213-w](https://doi.org/10.1007/s10796-021-10213-w).
- [18] M. Eswaran and M. R. Bahubalendruni, "Challenges and opportunities on AR/VR technologies for manufacturing systems in the context of industry 4.0: A state of the art review," *J. Manuf. Syst.*, vol. 65, pp. 260–278, 2022.
- [19] M. Eswaran, A. K. Gulivindala, A. K. Inkulu, and M. R. Bahubalendruni, "Augmented reality-based guidance in product assembly and maintenance/repair perspective: A state of the art review on challenges and opportunities," *Expert Sys. Appl.*, vol. 213, 2023, Art. no. 118983.
- [20] G. Wang, H. Liu, J. Luo, L. Mou, H. Pu, and J. Luo, "Reconstruction of smooth skin surface based on arbitrary distributed sparse point clouds," *IEEE Trans. Ind. Inf.*, vol. 19, no. 11, pp. 10663–10673, Nov. 2023.
- [21] M. Cao, L. Zheng, W. Jia, H. Lu, and X. Liu, "Accurate 3-D reconstruction under IoT environments and its applications to augmented reality," *IEEE Trans. Ind. Inf.*, vol. 17, no. 3, pp. 2090–2100, Mar. 2021.
- [22] F. Tao, M. Zhang, Y. Liu, and A. Y. Nee, "Digital twin driven prognostics and health management for complex equipment," *CIRP Ann.*, vol. 67, no. 1, pp. 169–172, 2018.



Wei Qiao received the B.E. degree in mechanical design, manufacturing, and automation in 2015 and the M.E. degree in control engineering, in 2018, from the Taiyuan University of Technology, Taiyuan, China, where she is currently working toward the Ph.D. degree in mechanical engineering.

Her research interests include machine vision and intelligent measurement.



Chengcheng Hou received the B.E. degree in information engineering from North Minzu University, Yinchuan, China, in 2011, and the M.E. degree in control engineering in 2021 from the Taiyuan University of Technology, Taiyuan, China, where he is currently working toward the Ph.D. degree in optical engineering.

From 2012 to 2018, he was an Electronics Engineer with the Shanxi Huida Sentechnics Co., Ltd, Taiyuan. His research interests include safety detection and energy-saving control of

transportation systems.



Xiaoyan Xiong received the Ph.D. degree in mechanical electronics engineering from the Taiyuan University of Technology, Taiyuan, China, in 2008.

She is currently a Professor with the Taiyuan University of Technology. She is the Vice Secretary General of dynamic testing committee of Chinese Vibration Engineering Society, and the Chairman of Shanxi Vibration Engineering Society. Her research interests include mechanical fault diagnosis, modern signal processing, and research on related software and hardware.



Huijie Dong (Member, IEEE) received the B.E. degree in automation from the University of Shanghai for Science and Technology, Shanghai, China, in 2013, and the Ph.D. degree in control theory and control engineering from the Institute of Automation, Chinese Academy of Sciences, Beijing, China, in 2022.

He is currently an Assistant Professor with the Key Laboratory of Advanced Transducers and Intelligent Control System, Ministry of Education, Taiyuan University of Technology, Taiyuan, China. His research interests include intelligent robots and perception.



Yusong Pang received the M.Sc. degree in electrical engineering from the Taiyuan University of Technology, Taiyuan, China, in 1996, and the Ph.D. degree in intelligent belt conveyor monitoring and control from the Delft University of Technology, Delft, The Netherlands, in 2007.

From 2000, he started working with Practic B.V. and Seaview B.V., The Netherlands, for industrial production life cycle management. After his Ph.D. research, he was employed with the Advisory Group Industrial Installations, Royal Haskoning, The Netherlands, in expert material handling. In 2010, he was appointed as Assistant Professor in transport engineering and logistics with the Delft University of Technology, The Netherlands. His research interests include the intelligent control for large-scale material handling systems and logistics processes.



Junzhi Yu (Fellow, IEEE) received the B.E. degree in safety engineering and the M.E. degree in precision instruments and mechanism from the North University of China, Taiyuan, China, in 1998 and 2001, respectively, and the Ph.D. degree in control theory and control engineering from the Institute of Automation, Chinese Academy of Sciences, Beijing, China, in 2003.

From 2004 to 2006, he was a Postdoctoral Research Fellow with the Center for Systems and Control, Peking University, Beijing. In 2006, he was an Associate Professor with the Institute of Automation, Chinese Academy of Sciences, where he became a Full Professor in 2012. In 2018, he joined the College of Engineering, Peking University, as a Tenured Full Professor. His current research interests include intelligent robots, motion control, and intelligent mechatronic systems.